Development 124, 2889-2901 (1997)
Printed in Great Britain © The Company of Biologists Limited 1997
DEV3560

An actin-mediated two-step mechanism is required for ventral enclosure of the *C. elegans* hypodermis

Ellen M. Williams-Masson[1], Amy N. Malik[2] and Jeff Hardin[1,2,*]

[1]Program in Cellular and Molecular Biology and [2]Department of Zoology, University of Wisconsin 1117 W. Johnson Street, Madison, WI 53706, USA

*Author for correspondence (e-mail: jdhardin@facstaff.wisc.edu)

SUMMARY

The epiboly of the *Caenorhabditis elegans* hypodermis involves the bilateral spreading of a thin epithelial sheet from the dorsal side around the embryo to meet at the ventral midline in a process known as ventral enclosure. We present evidence that ventral enclosure occurs in two major steps. The initial migration of the hypodermis is led by a quartet of cells, which exhibit protrusive activity at their medial tips and are required to pull the hypodermis around the equator of the embryo. These cells display actin-rich filopodia and treatment with cytochalasin D immediately halts ventral enclosure, as does laser inactivation of all four cells. Once the quartet of cells has migrated around the equator of the embryo and approaches the ventral midline, the remainder of the leading edge becomes visible on the ventral surface and exhibits a localization of actin microfilaments along the free edges of the cells, forming an actin ring. Cytochalasin D and laser inactivation block ventral enclosure at this later stage as well and, based upon phalloidin staining, we propose that the second half of enclosure is dependent upon a purse string mechanism, in which the actin ring contracts and pulls together the edges of the hypodermal sheet at the ventral midline. The ventral cells then form junctions with their contralateral neighbors to complete ventral enclosure.

Key words: epiboly, epithelium, morphogenesis, *Caenorhabditis elegans*, cell movement, actin, hypodermis

INTRODUCTION

The morphogenesis of epithelial tissues plays a fundamental role in animal development. Epithelial sheets fold, involute and migrate to give rise to internal structures during the processes of gastrulation, neurulation and organogenesis in vertebrates, and are responsible for lending structure and shape to invertebrate embryos (Trinkaus, 1984; Priess and Hirsh, 1986). Numerous in vitro and in vivo studies have been conducted in an effort to understand how epithelial sheets move and to identify the cellular components responsible for generating the morphogenetic forces required for epithelial morphogenesis.

One category of epithelial morphogenesis that has been investigated is the epiboly, or spreading, of epithelial sheets that have an advancing cell margin, or free edge. Numerous studies of wound healing have shown that large wounds made in cell monolayers heal by the extension of lamellipodia into the wound by border cells, and then subsequent migration of the border cells into the wound to seal the epithelial breach (Takeuchi, 1979, 1983; Radice, 1980; Gabbiani et al., 1978; Hergott et al., 1989; McCormack et al., 1992; Nusrat et al., 1992). Recent studies of avian embryonic skin epidermis and a cultured human intestinal cell line have shown that smaller wounds are capable of healing in the absence of lamellipodia via an actin-mediated concerted contraction that shrinks the wound perimeter (Martin and Lewis, 1992; Bement et al., 1993).

Another process that utilizes lamellipodia during epithelial movement is the morphogenesis of the epiblast, the outer cell layer of the blastoderm, during avian epiboly (Downie and Pegrum, 1971). The epiblast of the chick thins and spreads over the surface of the yolk, using the vitelline membrane as a migratory substratum. A strip of marginal cells three cells wide adheres strongly to the membrane and the free edge cells extend lamellipodia that are rich in actin microfilaments. The submarginal cells cannot migrate and are pulled passively by the migrating strip of marginal cells. During a functionally similar process, teleost epiboly, the enveloping layer flattens and spreads over the surface of the yolk. The contraction of a cortical microfilament meshwork within the yolk syncytial layer, coupled with cell rearrangement and narrowing of the enveloping layer marginal cells, has been postulated to be the driving force in the spreading of the enveloping layer (Betchaku and Trinkaus, 1978; Keller and Trinkaus, 1987).

The spreading of the preserosal epithelium to cover the honeybee embryo is an example of epiboly that does not utilize lamellipodia at the free edge (Fleig and Sander, 1988). Rather, the cells at the edge of the spreading preserosa exhibit blebbing and do not adhere to the substratum. Occasionally the marginal and submarginal cells change places, and serosal migration appears to be driven by the rearrangement and flattening of submarginal cells instead of active migration at the free edge. When the preserosa has almost completely enclosed the embryo, the free edges meet to form a circular ring, which then

closes by contracting like an iris diaphragm. A similar contraction has been observed during dorsal closure in *Drosophila*, as the epidermal layer spreads to enclose the embryo. Young et al. (1993) have shown that myosin and actin colocalize at the leading edge of the lateral cells during dorsal closure, and they postulated that these molecules provide the driving force in dorsal closure by contracting and pulling the edges of the epithelial sheet closed in a mechanism analogous to a purse string. Homozygous *zip* mutants, which possess mutations in the non-muscle myosin heavy chain, lack the localized myosin and fail to undergo dorsal closure.

Although the process of epiboly has been described in a variety of organisms, significant differences have been identified in the behavior of the migrating epithelial cells. The morphogenetic forces responsible for these movements have often remained unclear. In those model systems where it is possible to study morphogenetic forces (e.g. the chick), it is difficult to identify molecular players. Conversely, in systems amenable to molecular analysis, such as *Drosophila*, the experimental characterization of morphogenetic forces has been more difficult. In an effort to better understand the driving forces for epiboly, we have chosen to study the epiboly of the hypodermis during the process of ventral enclosure in the nematode *Caenorhabditis elegans*. The suitability of *C. elegans* for morphogenetic study was demonstrated by Priess and Hirsh (1986), who studied the role of the cytoskeleton in elongation of the embryo, a process that occurs immediately following ventral enclosure. They found that circumferential bands of microtubules and actin microfilaments are necessary for elongation and that disruption of these structures with pharmacological agents results in abnormal or aborted elongation.

In this study, we have characterized the role of the leading edge of the hypodermis as it spreads from the dorsal surface to enclose the embryo prior to its elongation. In addition, using laser microsurgery and pharmacological agents, we have investigated the forces necessary for enclosure and propose a two-step model for the generation of the forces necessary for successful ventral enclosure.

MATERIALS AND METHODS

Antibody staining

Embryos were obtained from gravid hermaphrodites via bleach treatment and rinsed in M9 solution (Sulston and Hodgkin, 1988). The embryos were attached to slides coated with 0.01% poly-L-lysine and processed for antibody staining by the freeze-cracking method (Sulston and Hodgkin, 1988). Briefly, coverslips were placed over the specimens and the slides were quick-frozen on dry ice. The coverslips were removed and the samples fixed in methanol and acetone, rehydrated through an acetone series and placed in PBS (125 mM NaCl; 16.6 mM Na_2HPO_4; 8.40 mM NaH_2PO_4) + 0.5% Tween-20 buffer (PBST). The specimens were incubated at 37°C for 1 hour in a 1:500 solution of MH27 antibody and PBST buffer + 1% dry milk (MH27 antibody recognizes a component of the adherens junction and was kindly provided by Dr R. Waterston, Washington University, St Louis, MO). The samples were rinsed in PBST buffer and incubated in a 1:25 solution of FITC-conjugated goat anti-mouse IgG for 30 minutes at 37°C. The samples were rinsed in PBST buffer and sealed in a drop of Slowfade anti-bleaching solution (Molecular Probes) and stored at 4°C. Laser scanning confocal microscopy was used to acquire serial optical sections and was performed at the Integrated Microscopy Resource, University of Wisconsin.

Nomarski time-lapse videomicroscopy

Gravid hermaphrodites were cut transversely through the vulva and the extruded embryos were mounted on a 5% agar pad in M9 solution. A coverslip was placed over the embryos and the mount was sealed with vaseline. Embryonic development was filmed using 4-D microscopy. The 4-D microscopy system consists of a Nikon Optiphot-II microscope equipped with differential interference contrast optics, a Z-axis stage controller operated via a Ludl Mac2000 control box and a Uniblitz electronic shutter on the transilluminator port. The shutter and Z-axis motor are controlled via serial cable connections to a Macintosh Quadra 950 computer equipped with a Scion LG3 8-bit frame grabber (Scion Corp., Frederick, MD), and device control and image acquisition are accomplished using a modified version of NIH Image. NIH Image is a public domain image analysis program written by Wayne Rasband available via anonymous ftp from zippy.nimh.nih.gov.

BODIPY 558/568 phalloidin staining

The following protocol is a modification of a protocol kindly provided by M. Costa at the Fred Hutchinson Cancer Research Center, Seattle, Washington (Costa et al., 1997). Gravid hermaphrodites were treated with a bleach solution as described above. The pellet was washed three times with M9 solution, then resuspended in 50 μl chitinase (Sigma) solution (5 units/ml chitinase in egg salts) and 1.5 ml egg salts. The embryos were incubated 5-10 minutes until hatching of pretzels and rounding up of the earlier stage embryos were observed. A formaldehyde/lysolecithin fix solution (42.4 mM Pipes, potassium salt, pH 6.8; 29.4 mM Hepes, pH 6.9; 11.8 mM EGTA; 2.4 mM $MgCl_2$; 117.6 mM lysolecithin, and 4.7% formaldehyde) was then added, the mixture vortexed and incubated 2 minutes at room temperature. The embryos were gently pelleted and resuspended in a formaldehyde fix solution (36 mM Pipes, potassium salt, pH 6.8; 25 mM Hepes, pH 6.9; 10 mM EGTA; 2 mM $MgCl_2$ and 4% formaldehyde) and agitated on a rocking platform for 25 minutes at room temperature.

The fixed embryos were pelleted, rinsed with 10 ml PBS + 0.1% Tween-20, and resuspended in PBS + 0.1% Tween-20 + 10 units/ml BODIPY 558/568 phalloidin (Molecular Probes). The embryos were agitated 1 hour at room temperature, then washed twice with PBS + 0.1% Tween-20 and once with PBS (10 minutes per wash). The embryos were mounted on frosted ring slides in Slowfade and viewed via confocal microscopy.

Scanning electron microscopy

Gravid hermaphrodites were treated with a bleach solution to obtain embryos as described above. The outer eggshell layer was removed by digestion with chitinase-chymotrypsin (Edgar, 1995) and the inner layer was removed by drawing the embryos through a pulled Pasteur pipette (Priess and Hirsh, 1986). The embryo solution was micropipetted onto coverslips precoated with 0.1% poly-L-lysine and allowed to settle for 15 minutes. Embryos were fixed in 2% glutaraldehyde and 2% formaldehyde in fixation buffer (0.15 M cacodylate buffer; 2 mM $MgSO_4$). Samples were washed in fixation buffer, dehydrated through an ethanol series and then critical-point dried (Ris, 1985). Specimens were coated with 1-2 nm of platinum and viewed with a Hitachi S-900 field-emission scanning electron microscope.

Laser ablations

Embryos were mounted as for time-lapse videomicroscopy. Laser ablations of individual cells were performed using a VSL-337ND nitrogen laser which was used to pump a tunable dye laser (Bull's Eye, Fryer Company) mounted on the stand of the Nikon Optiphot-II via a fiber optic conduit. Ablations were performed according to the procedures of Sulston and White (1980) and Avery and Horvitz (1989). Immediately following the ablation(s), the subsequent development of the embryos was documented by 4-D videomicroscopy.

Cytochalasin D experiments

Gravid hermaphrodites were cut at the vulva in water and the extruded embryos were mouth-pipetted onto coverslips precoated with 1 mg/ml poly-L-lysine. The embryos were allowed to settle 30 seconds and then treated 2 minutes with 100 μg of FITC-conjugated polylysine (Sigma). The embryos were rinsed three times with embryonic growth medium (EGM, Shelton and Bowerman, 1996) + 3 μg/ml Nile Blue A (Sigma) + 1-2 μg/ml cytochalasin D (EGMC), and covered with a 30 μl drop of EGMC. Stock solutions of 2 mg/ml cytochalasin D (Sigma) in DMSO were stored at 4°C. A ring of silicon oil was pipetted around the drop, four dots of silicon vacuum grease (Dow Corning) were placed at the corners of the coverslip to provide protective 'feet' and a slide was inverted over the coverslip to form the mount. The *C. elegans* eggshell is impermeable to the drug medium, so individual embryos were monitored via Nomarski microscopy. The eggshell was perforated by laser irradiation at the pertinent stage of development and the embryos were filmed by 4-D videomicroscopy. Embryos were scored 4 hours after permeabilization for blue gut granules, which indicated that sufficient permeabilization had been achieved for Nile Blue A penetration. In order to recover embryos for phalloidin staining, the coverslip was gently lifted from the mount following the laser perforation. The embryos were then processed for phalloidin staining as described above, beginning with the formaldehyde/lysolecithin fix step of the protocol.

RESULTS

Changes in the shape and position of hypodermal cells during enclosure

The hypodermis originates as a patch of cells at the posterior end of the dorsal side of the embryo. Immediately preceding ventral enclosure, the embryo undergoes dorsal intercalation on the dorsal side as two rows of dorsal hypodermal cells intercalate to form one elongated row of dorsal cells (Priess and Hirsh, 1986). Intercalation of the dorsal hypodermal cells is largely complete before the ventral marginal cells have migrated around the equator of the embryo, based on 3-dimensional MH27 immunostaining reconstructions and 4-D time-lapse videomicroscopy (E. Williams-Masson, P. Heid, C. Lavin and J. Hardin, unpublished data). During the process of ventral enclosure, the hypodermal tissue migrates laterally and ventrally to wrap the embryo in an epithelial monolayer. After ventral enclosure is complete, the anterior hypodermis encloses and the worm begins to elongate by constriction of actin microfilament bands that are circumferentially aligned. Lesions caused by laser irradiation during the process of elongation result in rupturing (Priess and Hirsh, 1986).

MH27 is an antibody that recognizes a component of the zonulae adherens and can thus be used to visualize epithelial boundaries within the hypodermis during enclosure (Podbilewicz and White, 1994). Staining of wild-type embryos reveals that, at the beginning of ventral enclosure, two anterior pairs of hypodermal cells lead the ventralward migration of the hypodermal sheet (Fig. 1A, arrows). Based upon previous descriptions of cell positions in the embryo (Sulston et al., 1983; Podbilewitz and White, 1994), this quartet of cells arises from the anterior blastomere of the 2-cell embryo, AB. Specifically, ABpraappap and ABpraapppa are the anterior and posterior leading right-hand hypodermal cells, and ABplaappap and ABplaapppa are the anterior and posterior leading left-hand hypodermal cells. We designate this quartet of cells to be the 'leading cells'; the anterior pair of cells eventually fuses after enclosure and forms part of the hyp6 hypodermal syncytium, and the posterior pair fuses and forms part of the hyp7 main body hypodermal syncytium (Fig. 10).

As these leading cells migrate around the equator of the embryo and begin moving toward the ventral midline, the hypodermal cells posterior to the leading cells become visible and the entire leading edge of the hypodermal sheet can be seen migrating toward the ventral midline (Fig. 1B). (In this lateral view only one side can be viewed of what is a bilateral process.) The ventral margin cells posterior to the leading cells include ABpraapppp and ABplaapppp, which will later fuse with hyp7, and the P cells, which are also descendants of the blastomere AB (Sulston et al., 1983). All of the hypodermal cells that comprise the leading edge of the hypodermis are

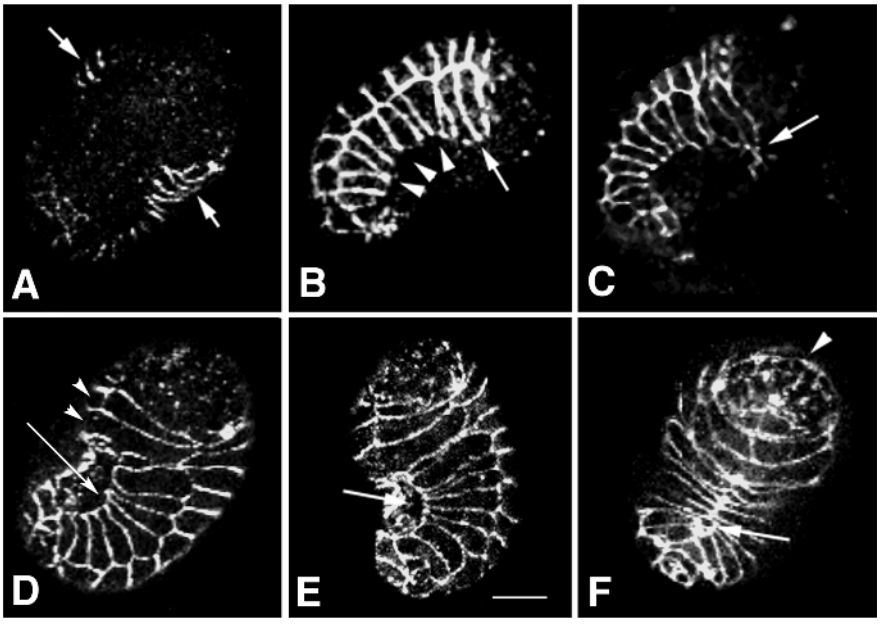

Fig. 1. Three-dimensional reconstructions of MH27 immunostaining of the ventral enclosure process in wild-type embryos collected by laser scanning confocal microscopy. (A) Ventral view of an embryo as the leading cells (arrows) first become visible on the ventral side. (B) Lateral view of leading cells (arrow) and the ventral pocket cells (arrowheads) slightly later in the ventral enclosure process. The free edges of the cells do not stain because MH27 only stains cellular junctions. (C) Ventrolateral view of the leading cells meeting at the ventral midline. The anterior pair of leading cells are the first to establish junctions (arrow). (D) Ventrolateral view of the ventral pocket (arrow) that is formed from the enclosing ventral marginal cells after the leading cells have met and formed junctions (arrowheads). The leading cells have changed in morphology, and have now acquired a rectangular shape. (E) The ventral pocket continues to enclose (arrow), becoming progressively smaller. Ventrolateral view. (F) The entire hypodermis has enclosed except for the tip of the anterior region (arrowhead) and a small ventral, posterior region (arrow). Ventral view; anterior is toward the top in all views. Bar, 10 μm.

elongated in the direction of migration. There is no MH27 staining at the free edges of the cells at the leading edge of the hypodermis (Fig. 1B), although the lateral borders of the cells are recognized by the antibody. The absence of staining at the free edges of the ventral margin cells is consistent with the MH27 antigen being present only at sites of cell-cell contact between epithelial cells.

The anterior-most pair of the quartet of leading cells reaches the ventral midline first and forms epithelial junctions (Fig. 1C, arrow). The other pair of leading cells then reaches the ventral midline and also forms junctions (Fig. 1D, arrowheads). At this stage of enclosure, the leading cells form rectangular strips as they meet at the midline, whereas the more posterior leading edge cells are more pointed in the direction of migration (Fig. 1D). By the time the quartet of leading cells have touched, the posterior leading edge cells have joined with the hypodermal cells wrapped around the posterior end of the embryo to form a 'ventral pocket', which proceeds to enclose (Fig. 1D,E, arrow). For clarity, we will refer to these more posterior ventral marginal cells as the 'ventral pocket' cells, and the leading cells and the ventral pocket cells will be referred to in aggregate as the 'ventral marginal' cells. Finally, all of the ventral hypodermal cells establish junctional connections with the corresponding contralateral cells. Thus, the ventral hypodermis 'zips up' at the ventral midline and the embryo assumes its characteristic bean shape (Fig. 1F). MH27 staining is now visible at the medial tips of the cells, indicating that the cells have formed junctions with their contralateral neighbors.

Nomarski time-lapse videomicroscopy of ventral enclosure

C. elegans embryos were mounted on agar pads and 4-D imaging was initiated approximately 2 hours before enclosure. Imaging of living embryos confirms that four ventral hypodermal cells (the leading cells) are the first cells of the hypodermal sheet to migrate around to the ventral side of the embryo (Fig. 2A,B, arrows). As these four cells migrate toward the ventral midline, the ventral pocket cells become visible as they migrate past the equator of the embryo and move toward the ventral midline (Fig. 2C, arrowheads; Fig. 2D, arrows). It is not possible to see all the leading edge cells in one image because they are in different focal planes; however, their relative position in living embryos can be ascertained using 4D videomicroscopy. 4D video-microscopy of ventral enclosure also allows for the estimation of rates of enclosure by the hypodermal sheet. From the time that the leading cells first become apparent on the ventral side, it takes them approximately 30 minutes to reach the ventral midline at 23°C; this corresponds to a migration rate of 0.3-0.4 μm/minutes. The ventral pocket cells, however, move at a much faster rate. Once they have become visible ventrally, it takes them approximately 10 minutes to reach the ventral midline, corresponding to a rate of 1.0-1.1 μm/minutes. Both of these rates are significantly slower than the rates of migration reported during chick (3.3-9.3 μm/min) and honeybee (7-10 μm/min) epiboly. During epiboly of embryos of *Fundulus* (a teleost fish), epithelial migration has been reported to range from 0.5-1.0 μm/min, which is similar to the migration rates reported here for *C. elegans* embryos.

Ventral enclosure is thus a fairly rapid process that is completed approximately 40 minutes after the leading cells first migrate past the equator of the embryo. The anterior region is the last part of the embryo to be enclosed by the hypodermal sheet, and appears to enclose via a mechanism distinct from ventral enclosure of the trunk and posterior, and is not addressed in this study.

Scanning electron microscopy of embryos undergoing ventral enclosure

Fig. 3A is a scanning electron micrograph of the lateral region of a pre-enclosure embryo which reveals the left-hand leading cells as they begin their migrations toward the ventral side of the embryo. The left-hand anterior leading cell is sending out three protrusions (see inset) from its ventral side and its

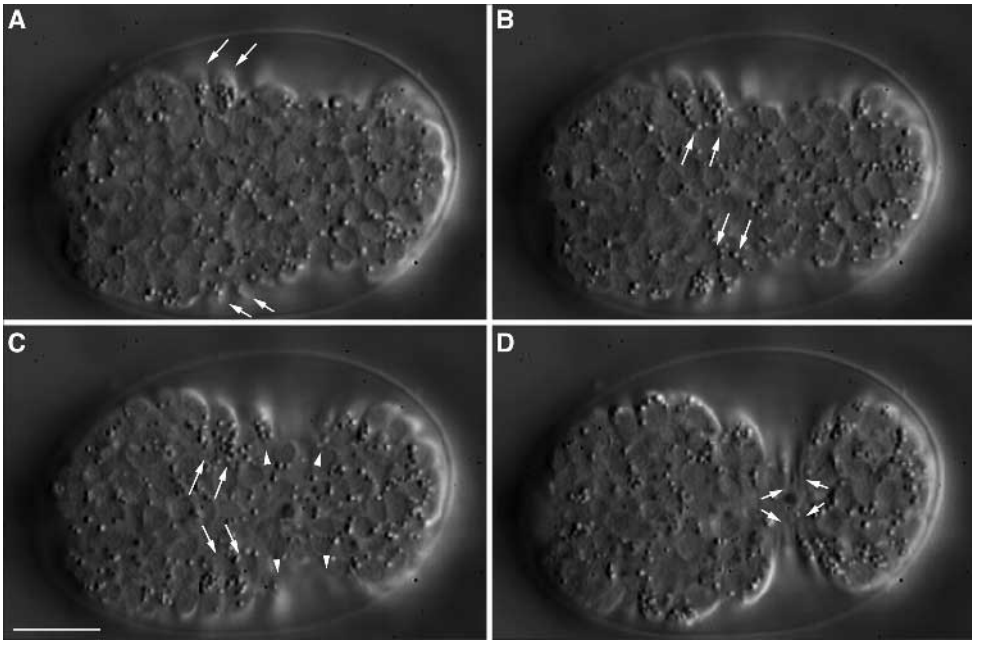

Fig. 2. Nomarski micrographs of ventral enclosure. (A) The four leading cells as they first become visible on the ventral surface of the embryo, and (B) migrate toward the ventral midline (arrows). (C) As the leading cells (arrows) approach the ventral midline, the ventral pocket cells become visible on the ventral surface (arrowheads). (D) The leading and ventral pocket cells (arrows) have enclosed. All views are ventral. Bar, 10 μm.

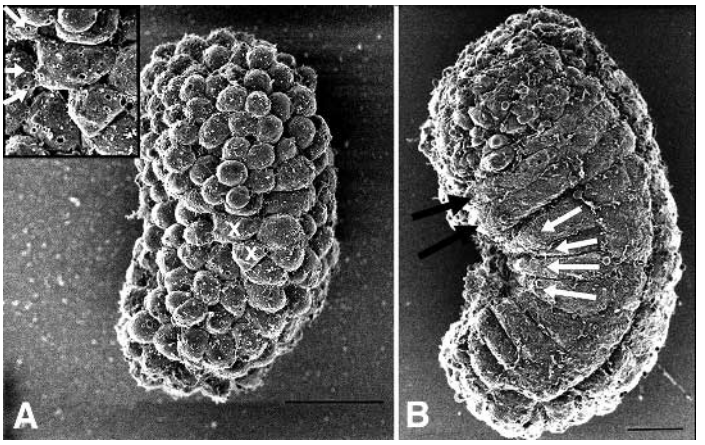

Fig. 3. Scanning electron micrographs of the early and late stages of ventral enclosure. (A) Lateral view of a pre-enclosure embryo showing the left-hand leading cells (X, and inset) as they begin migrating ventrally. Both cells have constricted back ends, and the anterior cell is extending three protrusions in the direction of migration (arrows, inset). (B) Lateral view of an enclosed embryo. The leading cells have met at the ventral midline, and have assumed a rectangular shape (black arrows). The ventral pocket cells have mostly enclosed, and have constricted ventral tips (white arrows). Anterior is toward the top, and dorsal is toward the right. Bar, 10 μm.

opposite end appears constricted. The left-hand posterior leading cell also has a constricted back end, but no large protrusions are yet visible.

Fig. 3B is a scanning micrograph of a lateral view of an embryo that has just completed the enclosure process. The left-hand leading cells have established connections with the right-hand leading cells and it appears that these cells have come together as elongated 'strips', with broad front and back ends (black arrows). In contrast, the ventral pocket cells have constricted ventral tips and this ventral constriction correlates with the ventral bending of the entire embryo (white arrows).

Laser inactivation of the leading cells

Laser irradiation of individual and groups of ventral marginal cells was performed to determine which cells are essential for migration of the hypodermal sheet during ventral enclosure. It is apparent that, when the ventral cells are irradiated, the cells are not completely killed; in experiments where the ventral cells are irradiated too severely, they immediately lyse and destroy the rest of the embryo. Thus, we believe that the ventral cells are not dead as a result of the irradiation, but that the irradiation instead causes the cells to round up and lose the ability to migrate, a process that we have termed 'laser inactivation'.

Cells were inactivated by laser irradiation of the cytoplasm of the migrating tip as soon as a migrating cell became visible in a ventral view, unless otherwise indicated. Embryos were subsequently scored for completion of ventral enclosure, rupture during elongation and successful elongation. Successful inactivation of a cell was scored as a cessation of migration. If a cell was irradiated too severely, the cell and subsequently the entire embryo lysed within minutes. Although the technique of laser irradiation has been widely applied in the study of *C. elegans* development (Bargmann and Avery, 1995), the specific physical effects of irradiation of cytoplasm are unclear. Thus we cannot rule out damage to the cellular junctions or the underlying extracellular matrix associated with an irradiated cell. However, in all experiments, no peripheral damage to adjacent cells was evident and only the irradiated cells were immediately affected in their ability to migrate.

In order to determine if the migration of the leading cells is required for the initial phase of ventral enclosure, the entire quartet of leading cells was irradiated as soon as the cells began migrating around the equator of the embryo. The inactivation of the leading cells resulted in immediate retraction (<10 seconds) of the hypodermal sheet back toward the dorsal side of the embryo in all cases (Fig. 4A,B). Any progress that the hypodermis had made in migrating toward the ventral midline was lost, as the entire hypodermis regressed dorsally. In 5 out of the 10 experiments performed, this retraction was permanent and the embryo was unable to reinitiate enclosure or undergo any elongation. However, in the other 5 experiments, the leading edge cells were able to reinitiate ventral enclosure. In these cases, ventral enclosure proceeded relatively normally, although it was somewhat delayed. There are apparently some defects in the enclosure process, however, as the embryos subsequently ruptured during elongation (Fig. 4C). It appears that the head remains enclosed to some degree, but the rest of the embryo ruptures under the internal pressure generated during elongation.

To determine if the leading cells are required for the completion of ventral enclosure, in two cases, the same four cells were inactivated 5-10 minutes later in enclosure, as the quartet of cells were approaching the ventral midline. In these cases, the hypodermis still retracted toward the dorsal side of the embryo; however, the leading cells were able to reinitiate enclosure, and the embryos completed ventral enclosure. The enclosure process was still flawed, but to a lesser degree, because in these experiments the embryos ruptured specifically in the ventral midsection. The head and tail were able to enclose and elongate successfully, but cells in the interior of the embryo were expelled through the small ventral rupture (Fig. 4D).

To determine if there is any coordination between the two pairs of leading cells during ventral enclosure, separate inactivations of the right-hand and left-hand pairs of the quartet of leading cells were performed. The right-hand pair of cells in Fig. 5 (white arrow) were inactivated as soon as they became visible on the ventral side, and rounded up and ceased migration within 1 minute of irradiation. The left-hand cells (Fig. 5, black arrow) were not affected in their ability to migrate and, upon reaching the ventral midline, continued migrating past the midline until they reached the inactivated right-hand cells. In all cases, these embryos completed ventral enclosure and elongated normally (n=5 right-hand ablations). A similar result was obtained when the left-hand cells were inactivated (n=4 left-hand ablations).

To test whether both leading cells are needed at a given axial position for successful enclosure and elongation, pairwise

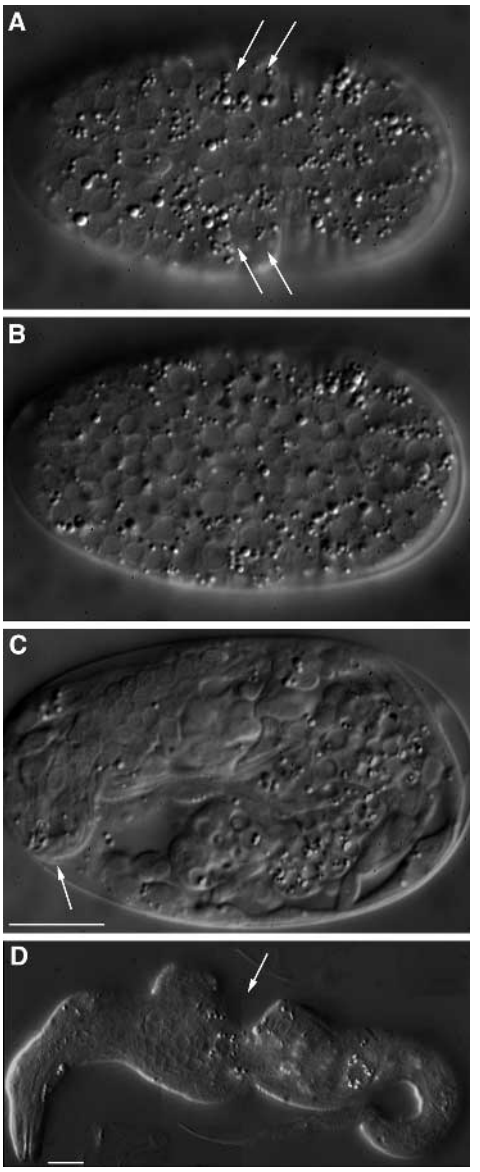

Fig. 4. Nomarski micrographs of embryos that had all four leading cells laser inactivated. (A) The four leading cells (arrows) were laser irradiated. (B) The hypodermis retracts back toward the dorsal side of the embryo. (C) In half the cases, as shown here, the hypodermis is able to reinitiate enclosure, but the embryo ruptures during elongation. The head is still partially intact (arrow). (D) Embryos that were irradiated slightly later in enclosure as the leading cells approached the ventral midline are able to reinitiate enclosure in all cases, but rupture specifically in the ventral region during elongation (arrow). All views are ventral; anterior is to the left. Bar, 10 μm.

ablations of right and left leading cells at the same antierior-posterior position were performed. First, the left and right anterior-most cells of the quartet of leading cells were inactivated. The embryos enclosed apparently normally yet, in all cases, they ruptured in the region of the irradiation during elongation (n=4; data not shown). Ablation of the left and right posterior pair (n=5), as well as diagonal ablations of the left anterior cell and the right posterior cell (n=5) gave similar results, with relatively normal enclosure, but region-specific

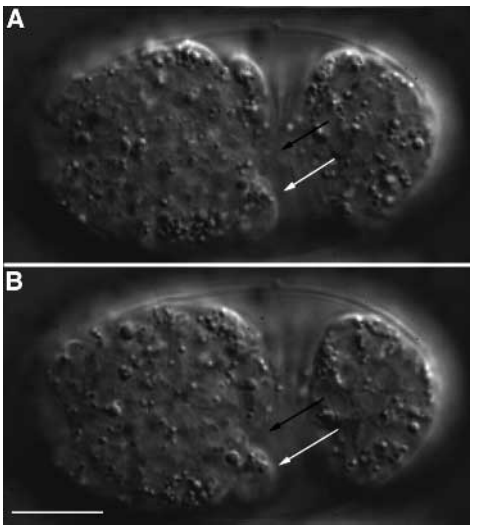

Fig. 5. Laser inactivation of the right-hand pair of leading cells. The posterior right and left-hand cells are in the plane of focus. (A) The right-hand leading cell (white arrow) ten minutes after laser irradiation. It has rounded up and ceased migrating. The left-hand leading cell has approached the ventral midline (black arrow). (B) The right-hand leading cell (white arrow) is still stationary, but the left-hand leading cell (black arrow) has extended past the ventral midline. Ventral view; anterior is to the left. Bar, 10 μm.

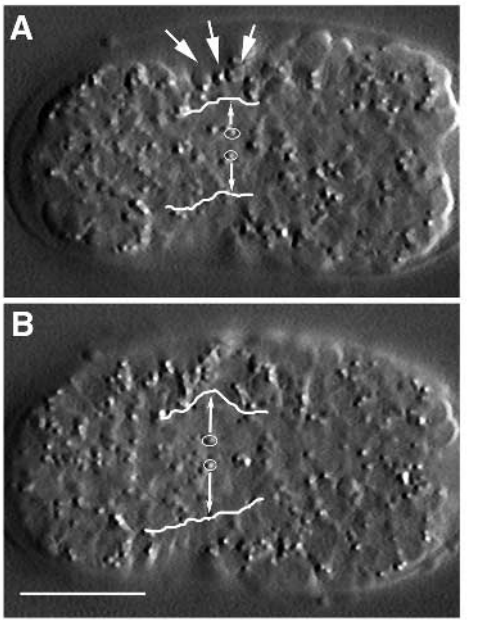

Fig. 6. Laser inactivation of the three anterior-most right-hand ventral pocket cells. The left and right margins of the hypodermis are indicated by curved lines. Yolk granules in underlying neuronal precursor cells serve as stationary landmarks, and are outlined by ellipses. For comparison between) and B, an arrow is drawn from each of these features extending to the left and right margins of the ventral hypodermis. (A) Three ventral pocket cells (arrows) were laser irradiated as they became visible on the ventral surface. (B) Same embryo as A, 25 seconds later. The hypodermis has begun retracting. Note that the unirradiated left side of the ventral pocket has also retracted. Ventral views; anterior is to the right. Bar, 10 μm.

Table 1 — Laser Inactivation of Leading Edge Cells

Inactivation§	*n*	Enclose	Elongate	Rupture¤	Ablation	*n*	Enclose	Elongate	Rupture
	10	YES* (No)	PARTIAL† (No)	YES* --		5	YES	PARTIAL	YES
	5	YES	YES	NO		5	YES	PARTIAL	YES
	4	YES	YES	NO		3	YES	YES	NO
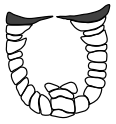	4	YES	PARTIAL	YES	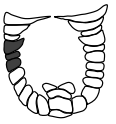	4	NO	NO	--

§The schematic diagrams shown here are intended to show which cells were inactivated, rather than the precise stage at which they were irradiated. All diagrams are schematic ventral views of the hypodermis. For details concerning the stage at which each class of inactivations was carried out, consult the Results. *n* represents the number of embryos in which the indicated cells were successfully inactivated. In all cases, unirradiated siblings in the same mount developed normally.

*Result in 5/10 experiments performed. Parentheses indicate the result in the remainder of cases.

†"Partial" elongation was defined as elongation to ≥ 1.5 fold, but less than full elongation.

¤"Rupture" denotes rupture of the embryo at a specific location along the anterior-posterior axis during elongation. Since embryos that fail to enclose do not elongate and cannot rupture, in these cases this category is not applicable (--).

ruptures during elongation. In all of these experiments, the anterior and posterior regions of the embryo appeared to be enclosed, but there were ruptures in the mid-sections of the developing embryos. These results are summarized in Table 1.

Laser inactivation of ventral pocket cells

The constricted apices of cells at the ventral margin of the hypodermis during mid- and late enclosure suggested that the ventral pocket may close via a purse-string-mediated contraction of its free edge. In order to test this idea, laser inactivation of the ventral pocket cells was performed. If the ventral pocket constricts by means of a purse string mechanism, then removing a segment of the purse string by irradiation would be expected to break the string and therefore block its closure. Inactivation of the three right-hand hypodermal cells immediately posterior to the leading cells caused an immediate retraction of the entire hypodermis within 30 seconds of irradiation (Fig. 6). The inactivation apparently caused a release of tension around the ventral hypodermal margin, because the nonirradiated contralateral ventral pocket cells showed a simultaneous, rapid retraction with respect to unenclosed neuronal precursor cells, which serve as stationary landmarks (Fig. 6B). Irradiated embryos were unable to reinitiate enclosure and subsequent hypodermal morphogenesis ceased in all cases (*n*=4). Surprisingly, inactivation of single ventral pocket cells did not have this effect; irradiated embryos continued to enclose and eventually elongated without rupturing in all cases (*n*=3). These results are summarized in Table 1.

Actin microfilament organization in the leading and ventral pocket cells

Because the leading edge of the ventral hypodermis displays motility and appears to mediate the enclosure process, we next examined the actin cytoskeleton of the leading cells and the ventral pocket cells using BODIPY 558/568 phalloidin and laser scanning confocal microscopy. Visualization of the quartet of leading cells revealed long, thin actin-rich protrusions extending from the tips of the cells toward the ventral midline (Fig. 7). These protrusions are not visible by Nomarski microscopy or MH27 staining, and appear to be migrating along the crevices of the boundaries between the neuronal precursor cells underneath them (Fig. 7A, arrows and arrowheads). Initially, the actin-rich filopodia extend predominantly from the anterior pair of the quartet (Fig. 7A). The posterior pair of cells also extend protrusions, but these filopodia connect to the anterior cells instead of extending toward the ventral midline directly (Fig. 7A,B). As the contralateral leading cells meet at the ventral midline, the actin tips overlap (Fig. 7B).

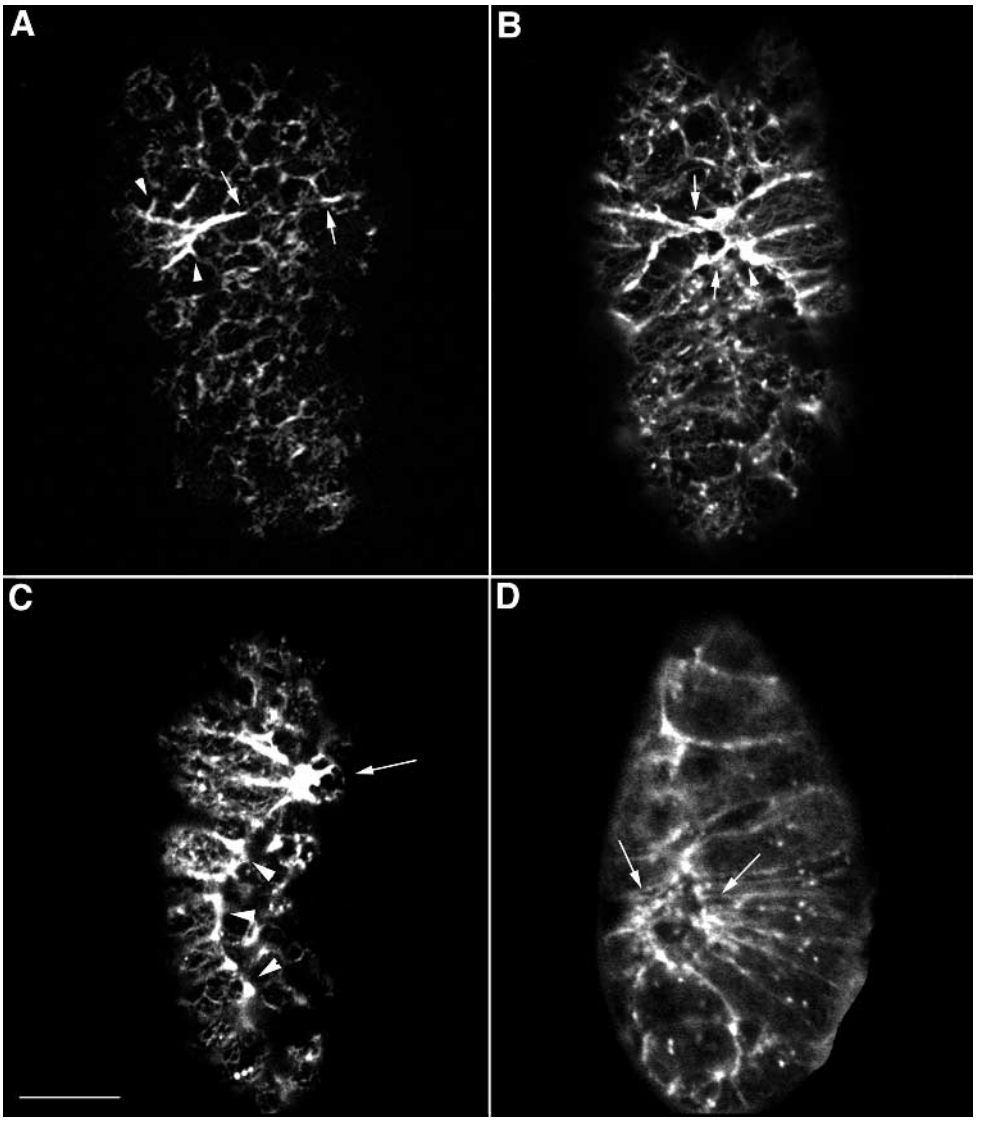

Fig. 7. Wild-type embryos stained with BODIPY-phalloidin and viewed by laser scanning confocal microscopy. (A) The anterior pair of leading cells exhibit long, actin-rich filopodia (arrows) as they migrate toward the ventral midline. Both pairs of leading cells also send out short, lateral filopodia (arrowheads). All of these filopodia appear to follow the cellular boundaries of the neuronal precursor cells underneath. (B) The filopodia of the leading cells meet and overlap at the ventral midline (arrows). Large amounts of localized actin can also be seen at the tips of the posterior leading cells (arrowhead). (C) As the leading cells begin to form junctions, large amounts of localized actin are visible at the tips of the leading cells (arrow). The ventral pocket cells also exhibit an increase in actin staining, and one side of the actin ring can be seen in this lateral view (arrowheads). (D) Ventral view of the ventral pocket as it is almost enclosed. The entire ring can be visualized (arrows). This embryo had been mounted in embryonic growth medium and laser permeabilized, then recovered and phalloidin stained. Thus, it does not stain as brightly overall as the other embryos, which were stained as described in the Methods. Bar, 10 μm.

When the leading cells form epithelial junctions, the actin bands at the epithelial junctions become thicker (Fig. 7C). The ventral pocket cells also exhibit actin localization along their ventral tips (Fig. 7C, arrowheads). These actin microfilaments appear to span the apical domain of each cell, forming a functionally continuous chain of actin that constricts as the ventral pocket closes (Fig. 7D, arrows).

Laser ablations of neuronal precursor cells under the migrating leading cells

Since the filopodia extended by leading cells appear to follow crevices between the underlying neuronal precursors, individual or small groups of neuronal precursors were ablated as the leading cells first became visible on the ventral surface and the results were analyzed via 4D microscopy (Fig. 8A). It is likely that ablation of the neuronal precursor cells often leads to damage of the thin filopodia of the overlying hypodermal cells, which cannot be seen via Nomarski microscopy. In these cases, the hypodermal cells often retract, or lyse (data not shown). However, it is possible to ablate neuronal precursor cells without harming leading cells if the ablation is done early enough during enclosure and the region of neuronal precursors damaged is not too large. In successful experiments where a small patch (1-3) of neuronal precursor cells was ablated and the leading cells were not damaged, the ablated neuronal precursor cells usually formed a mound of debris immediately after ablation (Fig. 8, white arrowhead). Based on analysis of time-lapse footage, translocation of other neuronal precursors to fill the space left by the extruded cells was restricted to at most one cell diameter. Since laser irradiation of neuronal precursor cells resulted in piles of dead cellular debris that were often completely extruded from the epithelium, these cells were not merely inactivated living cells as in the hypodermal laser inactivation experiments, but were truly ablated. The dead cells often shifted position or floated away when pushed upon by the migrating leading cells. In 7 of the 9 experiments performed, the leading cells migrated either over, under, or around the dead neuronal precursor area, the embryo enclosed normally and elongated (data not shown). In the other two experiments performed, the mound of debris formed by the neuronal precursor ablation appeared to physically block the migration of one pair of the leading cells, but the other

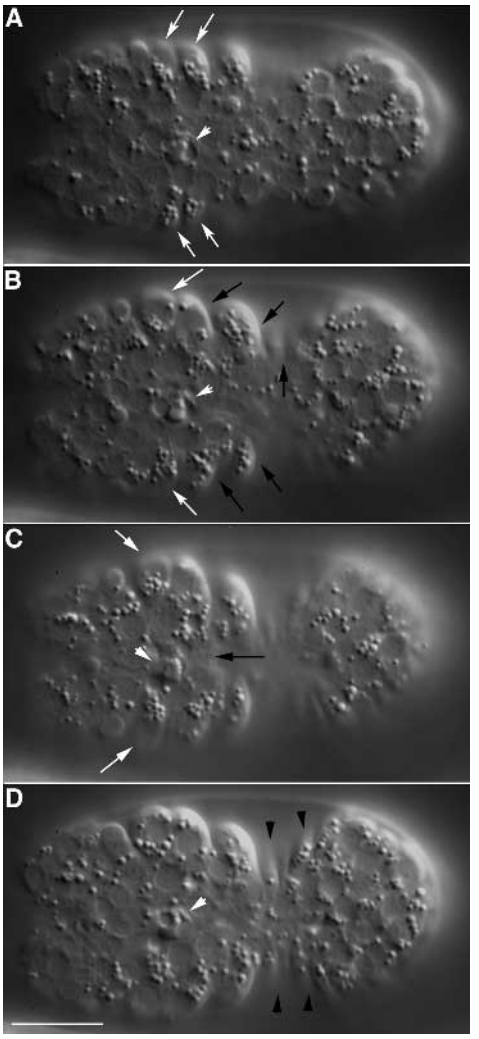

Fig. 8. Laser ablations of neuronal precursor cells underlying the migrating leading cells. (A) A small (2-3 cells) patch of neuronal precursor cells (arrowhead) was ablated as the leading cells (arrows) became visible on the ventral surface. (B) The anterior pair of leading cells (white arrows) become physically blocked during migration, although the other cells continue migrating (black arrows). (C) The posterior pair of leading cells (black arrow) have met at the ventral midline. The anterior pair of leading cells were unable to complete enclosure (white arrows). (D) Same timepoint, deeper focal plane. The ventral pocket cells have also enclosed (arrowheads). Ventral view, anterior is to the left. Bar, 10 μm.

ventral marginal cells moved around the obstacle and met normally at the ventral midline (Fig. 8B,C). In Fig. 8B, the anterior pair of leading cells (white arrows) was blocked by the mound of debris, but the more anterior pair of *hyp4* progenitor cells, the posterior pair of leading cells and the ventral pocket cells enclosed normally around the obstacle (Fig. 8C,D, black arrows and arrowheads).

Pharmacological disruption of actin structure during migration of the leading cells

As an initial functional test of the role of the actin cytoskeleton during ventral enclosure, wild-type embryos were mounted in EGMC medium containing 1 or 2 μg/ml cytochalasin D as described in the Materials and Methods and monitored via Nomarski microscopy. 1 μg/ml cytochalasin D has been shown to block elongation in *C. elegans* embryos (Priess and Hirsh, 1986). Embryos were permeabilized by laser irradiation of the eggshell as soon as the quartet of leading cells became visible on the ventral surface of the embryo (Fig. 9A). In all cases (n=5) the leading cells immediately ceased migration and often regressed toward the dorsal side of the embryo (Fig. 9B). The leading cells were never able to reinitiate enclosure and scoring of permeabilized embryos 4 hours later revealed staining of gut granules by Nile Blue A in the medium, verifying that complete permeabilization of the eggshell had been achieved. Some of the permeabilized embryos also exhibited muscular twitching, suggesting that exposure to these levels of cytochalasin D preferentially affects non-muscle motility. Control embryos permeabilized in EGM in the absence of cytochalasin D enclosed normally (data not shown).

Wild-type embryos mounted in EGMC were also laser permeabilized during the second stage of enclosure, after the leading cells had met at the ventral midline and the ventral pocket cells had moved past the equator of the embryo. In 5 of the 10 experiments performed, the ventral pocket cells had moved only a small distance past the equator when the embryos were laser permeabilized (Fig. 9C). In these cases, the ventral pocket cells stopped moving within about 20 minutes, and retracted toward the dorsal side of the embryo (Fig. 9D). In the remaining 5 cases, the embryos were laser permeabilized later during the second stage of enclosure, as the ventral pocket cells approached the ventral midline. In 3 out of 5 experiments, ventral pocket cell movement was not immediately halted (Fig. 9E,F). The ventral pocket cells continued to enclose, but at a very reduced rate and, by 45-70 minutes after the permeabilization, the cells did not appear to have formed junctions, as their tips were not touching at the ventral midline as in wild-type embryos and they had begun to retract. Within 2 hours, in all 3 of these embryos, the ventral pocket cells had retracted (Fig. 9G). In the remaining 2 embryos, permeabilized during late enclosure, the hypodermis retracted more rapidly, within 30-45 minutes. Blue gut staining indicated complete laser permeabilization was achieved in all cases. 2 of 10 embryos permeabilized midway through or late in the second stage of ventral enclosure developed a ‘pinhead’ phenotype. After the hypodermis retracted, the anterior region became constricted down to a small area, separated from the large posterior end of the embryo by a small ring of cells (Fig. 9H).

DISCUSSION

There are two distinct populations of ventral marginal cells during ventral enclosure

Various regions of the ventral hypodermis exhibit differences in morphology during ventral enclosure. A small group of cells at the anterior edge of the hypodermal sheet, the ‘leading cells’, are the first cells to migrate around the equator of the embryo and lead the progression of the entire hypodermal sheet toward the ventral midline. It is evident that these four cells exhibit filopodial activity at their medial tips and they appear to migrate actively from the initiation of ventral enclosure until they meet their contralateral partners and fuse at the ventral midline. In contrast to the quartet of leading cells, the ‘ventral

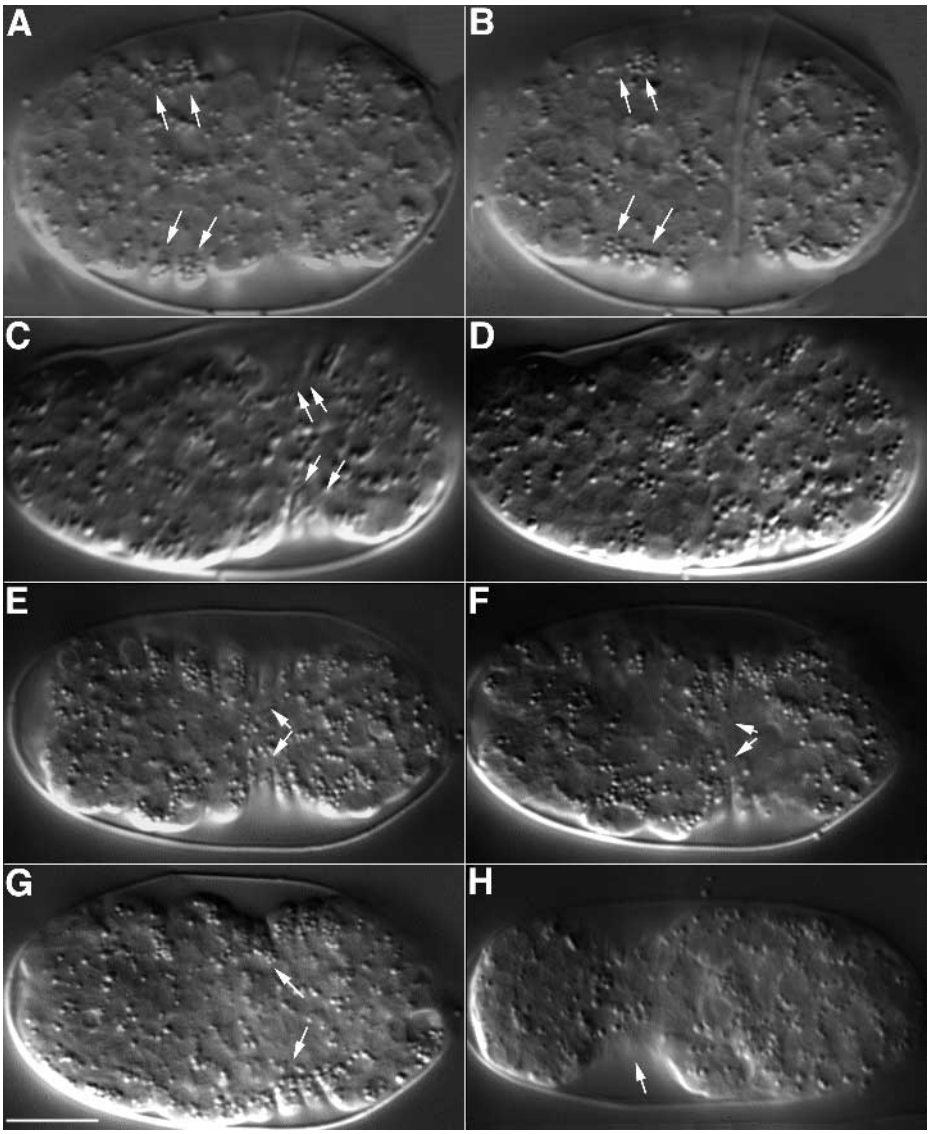

Fig. 9. Wild-type embryos exposed to the actin inhibitor cytochalasin D. Embryos were exposed to cytochalasin D during early (A,B), mid (C,D) and late (E-H) enclosure. (A) An embryo laser permeabilized as the quartet of leading cells first became visible on the ventral surface (arrows). (B) Same embryo, 10 minutes later. The leading cells immediately (within 1-2 minutes) ceased migrating, and often regressed toward the dorsal surface. (C) An embryo laser permeabilized after the leading cells had met at the ventral midline and the ventral pocket cells had begun migrating toward the ventral midline (arrows). (D) Within 10 minutes, the hypodermis had completely retracted. (E) An embryo laser permeabilized after the leading cells had met at the ventral midline and the ventral pocket cells had almost completely enclosed (arrows). (F) The ventral pocket cells gradually ceased migrating (arrows). After 45 minutes, the ventral pocket cells had still not completed enclosure. (G) Within 70 minutes, the ventral pocket cells had retracted toward the dorsal side (arrows). (H) The 'pinhead' phenotype was occasionally seen in these drug-treated embryos, as part of the embryo squeezed through a collar of joined hypodermal cells (arrow), leaving an embryo with a small anterior and a large, bulbous posterior. This collar of cells may be the leading cells, which appear to remain attached and do not retract with the rest of the hypodermis. Ventral views, anterior is to the left. Bar, 10 μm.

pocket' cells posterior to the leading cells do not have protrusive tips. The ventral pocket cells do, however, show a localization of actin along their free edges. This actin staining is detected in regions where MH27 is absent; this suggests that the actin ring does not require assembly of adherens-type junctions for its maintenance. There is no cell rearrangement along the ventral or lateral rows of cells; thus, cell rearrangement of these cells is not playing a role in driving *C. elegans* epiboly, as has been proposed for honeybee, teleost and chick epiboly.

'Leading cells' appear to initiate enclosure

Our laser ablation results make it probable that the quartet of leading cells is responsible for pulling the hypodermis from its initial position on the dorsal side past the equator of the embryo. If all four of the leading cells are laser inactivated early in enclosure, the entire hypodermis retracts back to the dorsal side of the embryo. In half the cases, the leading cells are able to reinitiate migration and the embryo encloses, although imperfectly. In the other half of the experiments, the hypodermis is unable to reinitiate enclosure. This variability may have several explanations. Ablation of leading cells during this stage of enclosure is technically difficult and it is possible that, in the cases in which enclosure was permanently blocked, irreparable damage to the entire embryo occurred. However, half of the embryos ablated during this stage of enclosure reinitiated enclosure coincident with the reinitiation of leading cell migration; this suggests that non-specific damage cannot account for all of the observed defects in enclosure due to leading cell irradiation. Alternatively, there may be variations in the reaction of the hypodermal cells to laser irradiation. In the cases where the hypodermis is able to reinitiate migration, the ventral cells presumably have sufficient time to recover from the irradiation and begin migrating again. That ruptures are seen in embryos that reinitiate enclosure during subsequent elongation suggests that the enclosure process is flawed. This may be due to a necessity for a temporal correlation between the various aspects of the enclosure process (i.e. the delay in leading cell migration may disrupt another step in enclosure). Alternatively, the irradiated cells may not be able to form appropriate junctions and therefore the hypodermis ruptures during elongation.

An inherent limitation of the laser inactivation approach is that the subcellular targets of laser irradiation are not known. Currently, there is little evidence for the presence of a well-developed basal lamina underlying the migrating hypodermal cells, either by transmission electron microscopy (E. Williams-Masson and C. Lavin, unpublished observations), or using available probes for typical basal laminar components, such as collagen (Kramer, 1994). However, we cannot rule out the presence of a thin extracellular matrix that may be disrupted by the laser. In addition, we cannot rule out an effect on the dorsal ends of these cells (i.e., the portion bounded by adherens junctional components) as a result of laser irradiation that subsequently disables the cell. Thus it is possible that the primary effect of inactivation is not on the protrusive appendages at the ventral edges of these cells. Whatever the primary effect of the laser, leading cell migration appears to be required for the further progression of the ventral margin of the hypodermis.

Exposure of embryos to the actin inhibitor cytochalasin D reveals roles for actin in the early phases of ventral enclosure. Embryos that were permeabilized during the first stage of enclosure were immediately affected, as the leading cells rounded up and, in many cases, retracted toward the dorsal side of the embryo. These experiments are consistent with the view that the actin-rich protrusions that are visible via phalloidin staining are necessary for the migration of the leading cells and that these protrusions are very sensitive to the concentrations of drug used in these experiments. Other explanations for the drug's effects, such as perturbation of underlying neuronal precursor cells, appear less likely. The neuronal precursors display no obvious motile activity in unperturbed embryos, based on scanning electron, transmission electron and 4-dimensional microscopy, as well as phalloidin staining.

Junction formation at the midline may be required to complete enclosure

The laser inactivation of axial pairs of cells and pairs of cells on the same side of the embryo reveal details of the requirement for junction formation during enclosure. If a pair of left-hand or right-hand cells is inactivated, the contralateral pair of cells migrates past the midline and the embryo is able to enclose and elongate. A healthy contralateral cell was able to extend past the midline and presumably form junctions with the inactivated cell, since the embryo was able to elongate without rupturing. When laser inactivation of both contralateral anterior or posterior cells is performed, the embryo erupts during elongation. This result is probably due to the inability of the two inactivated contralateral cells to form junctional complexes; the embryo then erupts at this spot as a result of the pressures generated during elongation. The inactivated cells face one another and, presumably, cannot breach the gap sufficiently to prevent eruption.

When a diagonal pair of cells (i.e. a left-hand anterior leading cell and a right-hand posterior cell) is inactivated, the embryo also erupts during elongation. It might be expected that the contralateral healthy cells would be able to overextend and bridge the gap across the ventral midline, but apparently this is not the case. Based on phalloidin staining and SEM, the posterior leading cells appear to migrate in part by their adherence to the anterior cells. Thus, in the diagonal inactivations, the healthy posterior cell may not be able to extend past the midline to its contralateral inactivated partner because its immediate anterior neighbor is inactivated and unable to contribute to the posterior cell's migration.

Leading cells are not dependent upon specific neuronal precursor cells for directional migration

Although the leading cells extend filopodia along the boundaries of the underlying neuronal precursor cells as they migrate, ablation of neuronal precursor cells directly in the path of migrating leading cells did not inhibit leading cell migration, except for cases where the neuronal precursor debris appeared to physically block the passage of leading cells. Therefore, it is unlikely that interactions between *specific* individual neuronal precursor cells and the migrating leading cells determine the direction of migration of the hypodermis; rather, the leading cells appear capable of migrating over neuronal precursor cells adjacent to the ablated neuronal precursor cells that would normally serve as their support. Since ablated neuronal precursors are extruded from the embryo, there is presumably a localized disruption of any extracellular matrix associated with the ablated cell(s), but this too appears insufficient to halt ventral migration of leading cells.

A two-step model for ventral enclosure: leading cell migration followed by purse string closure

We propose a two-step model for ventral enclosure that utilizes the two morphologically distinct groups of ventral hypodermal cells that we have described (Fig. 10). During the first step of enclosure, the right and left pairs of leading cells migrate around from the dorsal side of the embryo to meet at the ventral midline. As these leading cells migrate, they extend protrusions in the direction of migration. We propose that their migration generates tension, thereby pulling the remainder of the hypodermis around the equator of the embryo. The second stage of enclosure begins when the leading cells have nearly met at the ventral midline and the ventral pocket cells have been pulled around the equator of the embryo. We propose that the actin ring at the free edges of the ventral pocket acts to close the pocket, in a manner analogous to a purse string. Since the ventral pocket cells have already crested the widest diameter of the embryo, the actin ring is now able to constrict and bring the ventral pocket cells together at the ventral midline, where they form junctions with their contralateral neighbors. In this model, the correlation of these two events would be critical: if the actin ring constricts before the hypodermis migrates beyond the equator, the hypodermis would contract into a ball of cells on the dorsal side of the embryo, similar to that shown in Fig. 4.

Cytochalasin treatment during the second stage of enclosure is consistent with a purse string mechanism, since cytochalasin D is able to quickly inhibit enclosure of the ventral pocket during mid-enclosure. However, by late enclosure, the ventral pocket cells are not immediately halted. Because late enclosure occurs so rapidly (<10 minutes) and the actin purse string is so substantial at this point, there may be a delay before the effects of the drug can be seen. It is unlikely that the eventual retraction of the ventral pocket is a result of the embryo dying, since drug-treated embryos continue to twitch for a time beyond ventral pocket cell retraction. Analysis of dorsal closure in *Drosophila* has shown that purse string closure requires non-muscle myosin II function (Young et al., 1993). In these studies, actin and myosin were shown to colocalize at the

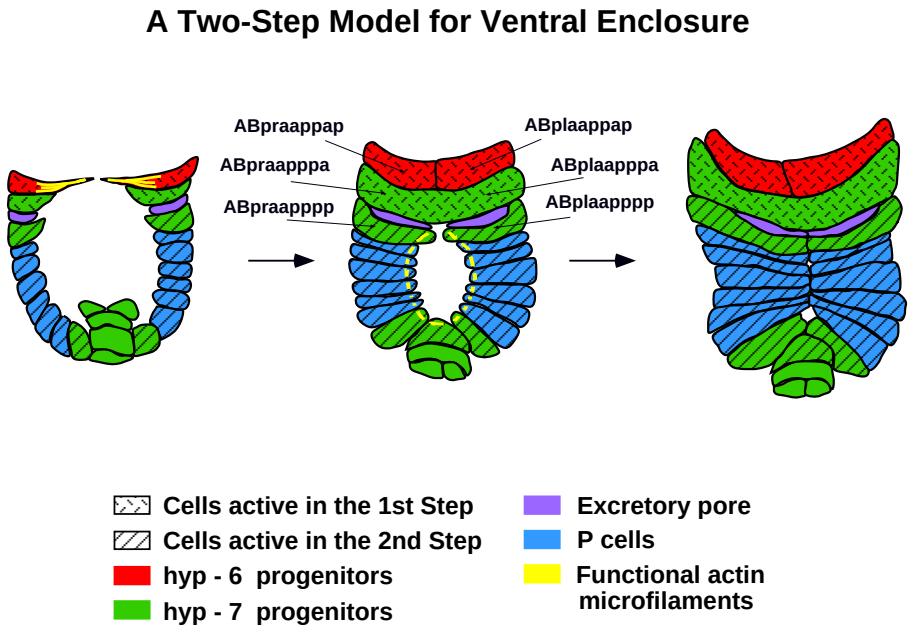

Fig. 10. Schematic diagrams of the two steps of ventral enclosure based upon a compilation of Nomarski microscopy, MH27 immunostaining, and phalloidin staining data. The stippled cells, the 'leading cells', are the cells involved in the first step of enclosure. The striped cells, the 'ventral pocket' cells, are the cells involved in the second step of enclosure. The various colors represent cells that generate various hypodermal tissues during later embryogenesis. The lineage designations of the cells that contribute to the hypodermal syncytia *hyp6* and *hyp7* are also shown in the middle diagram. The diagram at the left illustrates the position of the ventral marginal cells during the first step of enclosure, and shows the location of actin microfilaments mechanistically involved in this phase of morphogenesis (yellow). The middle diagram illustrates the position of the ventral marginal cells during the second step of ventral enclosure, and the location of the actin purse string (yellow), which is presumably required for this process. The diagram on the right shows the position of the ventral marginal cells after enclosure is complete. Ventral views, anterior is up in all figures.

leading edge of the epidermis and homozygous *zip* mutants lacking non-muscle myosin II failed to undergo dorsal closure. It is possible that a similar molecular motor plays a role during ventral enclosure in *C. elegans*, but this remains to be determined.

The inactivation of multiple ventral pocket cells also supports the purse string model. When three of the cells are inactivated, the hypodermis retracts immediately and bilaterally. This result is consistent with a release of tension around the free edges of the ventral pocket. The inactivation of one ventral pocket cell is insufficient for retraction, and is somewhat problematic for the purse string model. It may be that one cell can be extruded from the ventral pocket by neighboring cells without completely disrupting the continuity of the actin purse string. If the ventral pocket cells make transient attachments to underlying cells as the pocket closes, then removal of a single cell would be even less likely to irreversibly perturb purse string closure. Removal of three cells presumably causes a large enough gap in the ring to break the purse string irreversibly, and consequently the hypodermis retracts. Alternatively, the second stage of enclosure may occur by another, as yet unknown, mechanism, and inactivation of three cells along the ventral pocket may affect some aspect of ventral pocket closure other than force transmission around its free edge.

The relation of enclosure to subsequent morphogenesis in *C. elegans*

The successful completion of enclosure is crucial for the subsequent elongation of the embryo, which involves the constriction of circumferentially oriented bands of actin microfilaments (Priess and Hirsh, 1986). Based on phalloidin staining, these bands of actin become organized late in the enclosure process (E. W.-M., unpublished observation). It is possible that the circumferential tension generated during ventral enclosure helps to organize these bands. Alternatively, the lateral edges of dorsal and ventral hypodermal cells may in some way help organize the actin bands in the enclosed embryo, as microfilaments are parallel to the longitudinal cell boundaries of the hypodermal cells. In addition to alignment of cytoskeletal elements, junction formation along the ventral midline following enclosure is clearly a crucial requirement for successful elongation. Currently, this process is not well understood at the molecular level. A more detailed molecular understanding of ventral enclosure would be greatly facilitated by a genetic analysis of this process.

We are grateful to Jim Priess, Lois Edgar and Chris Shelton for technical advice on the laser permeabilization experiments and mounts; to Paul Heid for assistance setting up the mounts, and to John White, Patrick Masson, Paul Heid and Bill Raich for critical review of the manuscript. E. M. Williams-Masson was supported in part by funds from NIH Biotechnology Training Grant #GM08349. This work was also supported by a Lucille P. Markey Scholar Award in the Biomedical Sciences and a NSF Young Investigator Award to J. Hardin.

REFERENCES

Avery, L. and Horvitz, H. R. (1989). Pharyngeal pumping continues after laser killing of the pharyngeal nervous system of *C. elegans*. *Neuron* **3**, 473-485.

Bargmann, C. I. and Avery, L. (1995). Laser killing of cells in *Caenorhabditis elegans*. In *Caenorhabditis elegans: Modern Biological Analysis of an Organism* (ed. H. F. Epstein and D. C. Shakes), pp. 225-250. San Diego: Academic Press, Inc.

Bement, W. M., Forscher, P. and Mooseker, M. S. (1993). A novel cytoskeletal structure involved in purse string wound closure and cell polarity maintenance. *J. Cell Biol.* **121,** 565-578.

Betchaku, T. and Trinkaus, J. P. (1978). Contact relations, surface activity, and cortical microfilaments of marginal cells of the enveloping layer and of the yolk syncytial and yolk cytoplasmic layers of *Fundulus* before and during epiboly. *J. Exp. Zool.* **206**, 381-426.

Costa, M., Draper, B. W. and Priess, J. R. (1997). The role of actin filaments in patterning the Caenorhabditis elegans cuticle. *Dev. Biol.* **184**, 373-384.

Downie, J. R. and Pegrum, S. M. (1971). Organisation of the chick blastoderm edge. *J. Embryol. Exp. Morph.* **26**, 623-635.

Edgar, L. G. (1995). Blastomere culture and analysis. In *Caenorhabditis elegans: Modern Biological Analysis of an Organism* (ed. H. F. Epstein and D. C. Shakes), pp. 303-321. San Diego: Academic Press, Inc.

Fleig, R. and Sander, K. (1988). Honeybee morphogenesis: embryonic cell movements that shape the larval body. *Development* **103**, 525-534.

Gabbiani, G., Chaponnier, C. and Huttner, I. (1978). Cytoplasmic filaments and gap junctions in epithelial cells and myofibroblasts during wound healing. *J. Cell Biol.* **76**, 561-568.

Hergott, G. J., Sandig, M. and Kalnins, V. I. (1989). Cytoskeleton organization of migrating retinal pigment epithelial cells during wound healing in organ culture. *Cell Motil. Cytoskeleton* **13**, 83-93.

Keller, R. E. and Trinkaus, J. P. (1987). Rearrangement of enveloping layer cells without disruption of the epithelial permeability barrier as a factor in *Fundulus* epiboly. *Dev. Biol.* **120**, 12-24.

Kramer, J. (1994). Genetic analysis of extracellular matrix in *C. elegans*. *Ann. Rev. Genetics* **28**, 95-116.

Martin, P. and Lewis, J. (1992). Actin cables and epidermal movement in embryonic wound healing. *Nature* **360**, 179-183.

McCormack, S. A., Viar, M. J. and Johnson, L. R. (1992). Migration of IEC-6 cells: a model for mucosal healing. *Am. J. Physiol.* **263**, G426-435.

Nusrat, A., Delp, C. and Madara, J. L. (1992). Intestinal epithelial restitution. Characterization of a cell culture model and mapping of cytoskeletal elements in migrating cells. *J. Clin. Invest.* **89**,1501-1511.

Podbilewicz, B. and White, J. G. (1994). Cell fusions in the developing epithelia of *C. elegans*. *Dev. Biol*. **161**, 408-424.

Priess, J. R. and Hirsh, D. I. (1986). *Caenorhabditis elegans* morphogenesis: The role of the cytoskeleton in elongation of the embryo. *Dev. Biol.* **117**, 156-173.

Radice, G. P. (1980). The spreading of epithelial cells during wound closure in *Xenopus* larvae. *Dev. Biol.* **76**, 26-46.

Ris, H. (1985). The cytoplasmic filament system in critical-point dried whole mounts and plastic-embedded sections. *J. Cell Biol.* **100**, 1474-1487.

Shelton, C. A. and Bowerman, B. (1996). Time-dependent responses to *glp-1*-mediated inductions in early *C. elegans* embryos. *Development* **122,** 2043-2050.

Sulston, J. E. and Hodgkin, J. (1988). Methods. In *The Nematode Caenorhabditis elegans* (ed. W. B. Wood), pp 587-606. New York: Cold Spring Harbor Laboratory Press.

Sulston, J. E., Schierenberg, E., White, J. G. and Thomson, J. N. (1983). The embryonic cell lineage of the nematode *Caenorhabditis elegans*. *Dev. Biol*. **100**, 64-119.

Sulston, J. E. and White, J. G. (1980). Regulation and cell autonomy during postembryonic development of *Caenorhabditis elegans*. *Dev. Biol.* **78**, 577-597.

Takeuchi, S. (1979). Wound healing in the cornea of the chick embryo IV. Promotion of the migratory activity of isolated corneal epithelium in culture by the application of tension. *Dev. Biol*. **70**, 232-240.

Takeuchi, S. (1983). Wound healing in the cornea of the chick embryo V. An observation and quantitative assessment of the cell shapes in isolated corneal epithelium during spreading in vitro. *Cell Tissue Res.* **229**, 109-127.

Trinkaus, J. P. (1984). *Cells into Organs- The Forces that Shape the Embryo*. Englewood Cliffs, New Jersey: Prentice Hall.

Young, P. E., Richman, A. M., Ketchum, A. S. and Kiehart, D. P. (1993). Morphogenesis in *Drosophila* requires nonmuscle myosin heavy chain function. *Genes Dev.* **7,** 29-41.

(Accepted 2 June 1997)